

## Dynamic relaxation characteristics of Matrimid<sup>®</sup> polyimide

Anthony C. Comer<sup>a</sup>, Douglass S. Kalika<sup>a,\*</sup>, Brandon W. Rowe<sup>b,c</sup>, Benny D. Freeman<sup>b,c</sup>, Donald R. Paul<sup>b</sup>

<sup>a</sup> Department of Chemical and Materials Engineering, University of Kentucky, Lexington, KY 40506-0046, USA

<sup>b</sup> Department of Chemical Engineering and Texas Materials Institute, The University of Texas at Austin, Austin, TX 78712, USA

<sup>c</sup> Center for Energy and Environmental Resources, Department of Chemical Engineering, The University of Texas at Austin, Austin, TX 78758, USA

### ARTICLE INFO

#### Article history:

Received 30 July 2008

Received in revised form

2 December 2008

Accepted 7 December 2008

Available online 11 December 2008

#### Keywords:

Dynamic mechanical analysis

Dielectric spectroscopy

Physical aging

### ABSTRACT

The dynamic relaxation characteristics of Matrimid<sup>®</sup> (BTDA–DAPI) polyimide have been investigated using dynamic mechanical and dielectric methods. Matrimid exhibits three motional processes with increasing temperature: two sub-glass relaxations ( $\gamma$  and  $\beta$  transitions), and the glass–rubber ( $\alpha$ ) transition. The low-temperature  $\gamma$  transition is purely non-cooperative, and displays an identical time–temperature response to both the dynamic mechanical and the dielectric probes with a corresponding activation energy,  $E_A = 43$  kJ/mol. The  $\beta$  sub-glass transition shows a more cooperative character as assessed via the Starkweather method. Comparison of dynamic mechanical and dielectric data for the  $\beta$  process suggests that the dynamic mechanical test ( $E_A = 156$  kJ/mol) is sensitive to a broader, more strongly correlated range of sub-glass motions as compared to the dielectric probe ( $E_A = 99$  kJ/mol). Time–temperature superposition was used to establish mechanical master curves across the glass–rubber ( $\alpha$ ) relaxation, and these data could be described using the Kohlrausch–Williams–Watts function with an exponent value,  $\beta_{KWW} = 0.34$ . The corresponding shift factors were used as the basis of a cooperativity plot for the determination of dynamic fragility. The relation between fragility index ( $m = 115$ ) and  $\beta_{KWW}$  for the Matrimid polyimide was in good agreement with the wide correlation reported in the literature.

© 2008 Elsevier Ltd. All rights reserved.

## 1. Introduction

Polymers below their glass transition temperature,  $T_g$ , are non-equilibrium materials that evolve over time towards an equilibrium state. This process, known as physical aging, is manifested by changes in physical properties of the polymer and has been studied extensively for bulk materials [1–3]. Physical aging is strongly dependent on the system temperature, which affects both segmental mobility and displacement from equilibrium [4]. Molecular motions that persist below the glass transition, related to secondary transitions, allow physical aging to proceed by small localized rearrangements towards equilibrium [2].

It has been suggested that physical aging does not continue at temperatures below the sub-glass transition range, because the localized motions related to these processes become frozen. However, evidence of low-temperature aging (*i.e.*, below the sub-glass transition) has been reported [5,6]. For example, Lee and

McGarry showed that cooperative segmental motions exist at temperatures below  $T_g$  in polystyrene, as evidenced by isothermal volume relaxation [6]. By studying the effect of secondary relaxations on physical aging, additional insight regarding the molecular mechanisms responsible for aging may be obtained and improved performance predictions, as well as strategies to control and possibly arrest physical aging, can be developed.

Matrimid<sup>®</sup> is a high  $T_g$ , amorphous thermoplastic polyimide comprised of 3,3'-4,4'-benzophenone tetracarboxylic dianhydride (BTDA) and diaminophenylindane (DAPI); see Fig. 1 [7]. Matrimid is a useful material for the creation of gas separation membranes [8–10]. However, the performance of these membranes decreases over time due to physical aging [11–13]. In an effort to more fully understand the mechanisms responsible for physical aging in the BTDA–DAPI polyimide, a comprehensive study of the dynamic relaxation characteristics of the commercial polymer has been undertaken. Specifically, dynamic mechanical analysis (DMA) and broadband dielectric spectroscopy (BDS) have been used to determine the glass–rubber and sub-glass transition properties of the Matrimid polyimide. This detailed investigation provides valuable information regarding the nature of the underlying motional processes responsible for these transitions, and their potential relationship to physical aging.

\* Corresponding author. Department of Chemical and Materials Engineering, University of Kentucky, 177 Anderson Hall (Tower), Lexington, KY 40506-0046, USA. Tel.: +1 859 257 5507; fax: +1 859 323 1929.

E-mail address: [kalika@engr.uky.edu](mailto:kalika@engr.uky.edu) (D.S. Kalika).

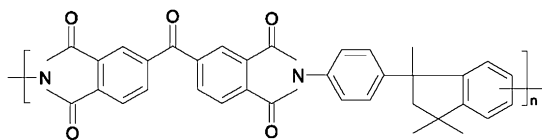


Fig. 1. Chemical structure of Matrimid® BTDA-DAPI (3,3'-4,4'-benzophenone tetra-carboxylic dianhydride and diaminophenylindane) polyimide.

Characterization of the dynamic relaxation processes of polyimides as a function of constituent backbone structure has been an area of extensive activity. Dynamic mechanical and dielectric relaxation techniques have been widely applied to establish transition temperatures, relative relaxation intensity, and the time-temperature characteristics of the motional transitions encountered in these materials [14–28]. To date, however, a detailed report of the sub-glass and glass-rubber relaxation properties of BTDA-DAPI (i.e., Matrimid) has not appeared.

A number of authors have summarized the common relaxation features of polyimides [22,26,28]. Typically, three relaxation processes are observed with increasing temperature designated  $\gamma$ ,  $\beta$  and  $\alpha$ , respectively, with  $\alpha$  corresponding to the glass-rubber relaxation. For polyimides based on the BTDA dianhydride,  $T_\gamma$  (re: dynamic mechanical peak at 1 Hz) is usually in the vicinity of  $-110$  to  $-90$  °C, and  $T_\beta$  is observed at  $80$ – $130$  °C [23,28]. Owing to the local character of the sub-glass relaxations, their time-temperature relations can be described by a constant activation energy according to the Arrhenius relation. For the  $\gamma$  process, the apparent activation energy ( $E_A$ ) is approximately  $40$ – $60$  kJ/mol, and for the  $\beta$  process,  $E_A = 130$ – $160$  kJ/mol. While the  $\gamma$  and  $\beta$  sub-glass relaxations are nominally local and non-cooperative in nature, the exact molecular mechanisms underlying these relaxations have been the subject of some discussion [22]. In the case of the  $\gamma$  transition, the presence of residual water in the polymer appears to play an important role, with numerous studies reporting a direct correlation between water content and the intensity of the relaxation [15,16,28]. However, there is sufficient evidence to suggest that for many systems, detection of the  $\gamma$  transition is not solely dependent on the presence of coupled water molecules, and may reflect limited motions such as phenyl ring oscillations [20,22]. For the  $\beta$  transition in polyimides, various mechanisms have been postulated involving motions that while still essentially local in character, encompass larger portions of the repeat unit that respond in a correlated manner [17,18,22]. A recent review by Ngai and Paluch examines in detail the dynamic properties of sub-glass relaxations, and in particular the characteristics of secondary relaxations in glass formers with varying degrees of flexibility. In more rigid systems, the origin of the  $\beta$  relaxation is linked to small amplitude motions that ultimately involve the entire repeat segment [29].

## 2. Experimental

### 2.1. Materials

Commercial polyimide based on 3,3'-4,4'-benzophenone tetra-carboxylic dianhydride and diaminophenylindane (BTDA-DAPI; Matrimid® 5218 from Huntsman Advanced Materials) was generously supplied by Air Liquide/Medal, Newport, DE. The polymer was provided in the form of flakes, and was used as-received in this study. The structure of Matrimid is shown in Fig. 1.

### 2.2. Film preparation

Polymer films (thickness of  $\sim 150$   $\mu\text{m}$ ) were prepared by solution casting onto silicon wafers using metal casting rings. The

casting solvent was methylene chloride and glass plates were used as covers to slow evaporation. The films were allowed to dry for one week at ambient conditions and were subsequently held under vacuum at  $100$  °C for four days,  $200$  °C for one day, and then in a nitrogen purge at  $330$  °C for 30 min. This drying procedure was designed to maximize solvent removal without crosslinking the material, which can occur when the polymer is exposed to high temperatures in the vicinity of  $T_g$  for extended times [30]. Solubility tests performed on samples subjected to the drying protocol indicated no evidence of crosslinking. Upon completion of the solvent-removal procedure, the samples were stored at ambient temperature and humidity. Prior studies on water uptake in annealed Matrimid films indicate an equilibrium water content of approximately 1.5 wt% for these test samples (50% relative humidity, see Ref. [31]).

### 2.3. Dynamic mechanical analysis

Dynamic mechanical analysis was performed using a TA Instruments Q800 DMA configured in tensile geometry. Storage and loss moduli ( $E'$ ;  $E''$ ) were measured both in temperature sweep mode (1 Hz;  $3$  °C/min), as well as in frequency sweep mode ( $0.1$ – $30$  Hz) at discrete temperatures ranging from  $-150$  to  $425$  °C. All measurements were performed under nitrogen atmosphere.

### 2.4. Broadband dielectric spectroscopy

Dielectric spectroscopy was performed using the Novocontrol "Concept 40" broadband dielectric spectrometer (Hundsangen, Germany). Prior to measurement, concentric silver electrodes were vacuum-evaporated on each polymer sample using a VEECO thermal evaporation system. Samples were subsequently mounted between gold platens and positioned in the Novocontrol Quatro Cryosystem. Dielectric constant ( $\epsilon'$ ) and loss ( $\epsilon''$ ) were recorded in the frequency domain (1 Hz–1 MHz) at  $10$  °C isothermal intervals from  $-150$  to  $300$  °C (i.e., sub-glass transition range). A high level of conduction was encountered at temperatures  $>300$  °C, precluding a full analysis of the glass-rubber relaxation via dielectric methods.

## 3. Results and discussion

### 3.1. Relaxation properties of Matrimid polyimide

The overall dynamic mechanical relaxation properties of the BTDA-DAPI polyimide are reported as storage and loss moduli (1 Hz) vs. temperature in Fig. 2. Matrimid shows three distinct

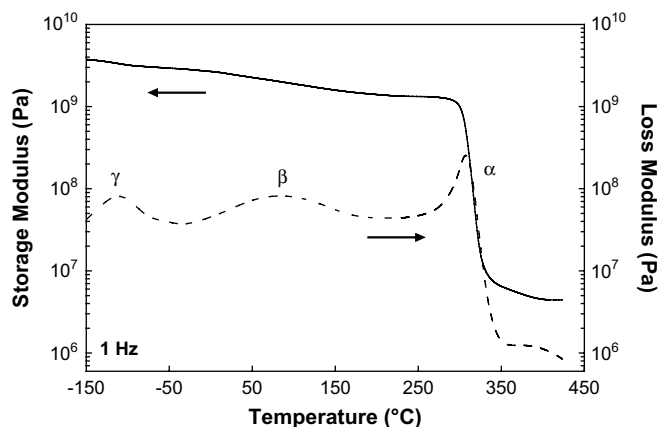


Fig. 2. Storage modulus (—, Pa) and loss modulus (---, Pa) vs. temperature (°C) for Matrimid® polyimide. Frequency of 1 Hz, heating rate of  $3$  °C/min.

relaxation peaks in  $E''$  with increasing temperature, consistent with the results for similar polymers [28]; the relaxations are labeled as  $\gamma$ ,  $\beta$  and  $\alpha$ , respectively, where  $\alpha$  corresponds to the glass transition. The peak temperatures are:  $-112^\circ\text{C}$  ( $T_\gamma$ ),  $80^\circ\text{C}$  ( $T_\beta$ ) and  $313^\circ\text{C}$  ( $T_\alpha$ ). Dielectric loss data ( $\epsilon''$ ) are compared with the mechanical loss results across the sub-glass transition range in Fig. 3. The dielectric results also show two distinct sub-glass transitions, and the position and breadth of each relaxation are in close correspondence to the dynamic mechanical curve. Based on the relative peak heights of the sub-glass transitions, the  $\beta$  process would appear to be somewhat more prominent in the dynamic mechanical measurement.

### 3.2. Sub-glass relaxation processes

Detailed dynamic mechanical results for the  $\gamma$  and  $\beta$  transitions (0.1–30 Hz) are presented in Fig. 4; please note the different temperature scales associated with the individual graphs. The maxima in  $E''$  from the isochronal curves are the basis for the Arrhenius plots ( $f$  [Hz] vs.  $1000/T$  [K]) presented in Fig. 5. Over the limited range of accessible frequencies, both the  $\gamma$  and the  $\beta$  dynamic mechanical data sets display linear Arrhenius behavior. The slope of the data reflects the apparent activation energy in each case:  $E_A(\gamma) = 43$  kJ/mol and  $E_A(\beta) = 156$  kJ/mol. These values are in good agreement with the ranges reported for polyimides based on BTDA, as discussed above [28].

Dielectric data for the  $\gamma$  and  $\beta$  transitions are presented as dielectric loss vs. frequency at discrete temperatures in Fig. 6. The individual relaxations can be described using the Havriliak–Negami (HN) modification of the single-relaxation time Debye expression:

$$\epsilon^* = \epsilon' - i\epsilon'' = \epsilon_U + \frac{\epsilon_R - \epsilon_U}{[1 + (i\omega\tau_{\text{HN}})^a]^b} \quad (1)$$

where  $\epsilon_R$  and  $\epsilon_U$  represent the relaxed ( $\omega \rightarrow 0$ ) and unrelaxed ( $\omega \rightarrow \infty$ ) values of the dielectric constant for each relaxation,  $\omega = 2\pi f$  is the frequency,  $\tau_{\text{HN}}$  is the relaxation time for each process, and  $a$  and  $b$  represent the broadening and skewing parameters, respectively [32,33]. When the parameters  $a = b = 1$ , Eq. (1) reverts to the Debye form. The WINFIT software package provided with the Novocontrol spectrometer was used to obtain HN best fits for the  $\epsilon''$  vs. frequency data at each temperature; see solid curves in Fig. 6. HN parameters determined for the individual relaxations are plotted vs. temperature in Fig. 7, with  $\Delta\epsilon = \epsilon_R - \epsilon_U$  corresponding to the dielectric relaxation intensity. For the sub-glass  $\gamma$  transition, both

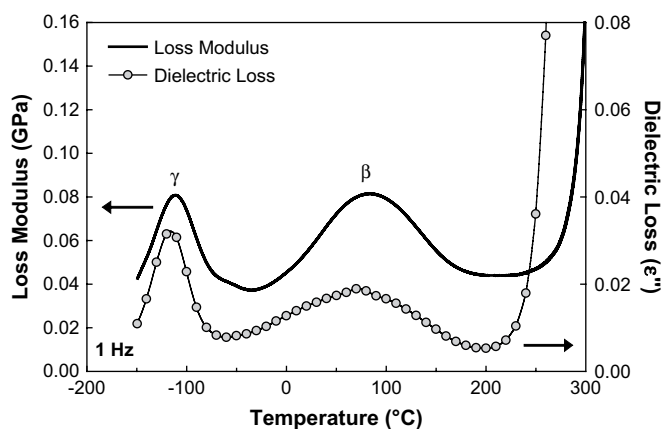


Fig. 3. Dynamic mechanical loss modulus (—, GPa) and dielectric loss (●) vs. temperature ( $^\circ\text{C}$ ) for Matrimid® polyimide across the sub-glass transition region. Frequency of 1 Hz.

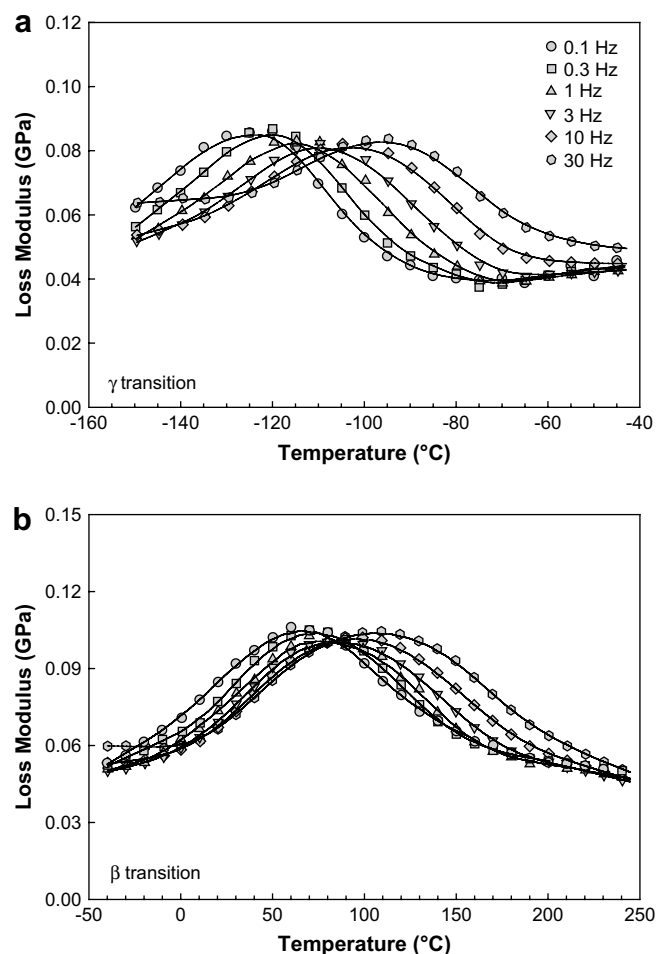


Fig. 4. Loss modulus (GPa) vs. temperature ( $^\circ\text{C}$ ) for Matrimid® polyimide. (a)  $\gamma$  transition; (b)  $\beta$  transition. Curves are provided as a guide to the eye.

broadening and high-frequency skewing are evident, with  $a \sim 0.5$  and  $b \sim 0.4$ , respectively. In the case of the  $\beta$  transition, the dielectric dispersion is observed to be symmetric in the frequency domain, such that the data can be satisfactorily fit using the Cole–Cole form of Eq. (1), with the skewing parameter ( $b$ ) equal to unity [34]. The  $\beta$  relaxation is observed to narrow with increasing temperature (i.e., broadening exponent ( $a$ ) increases with temperature), indicating a tighter distribution of relaxation times at higher temperature. The relaxation intensity ( $\Delta\epsilon$ ) is comparable in magnitude for both sub-glass relaxations, and decreases with temperature reflecting an apparent loss of net dipolar correlation with increasing thermal energy.

Relaxation times associated with the individual dielectric dispersions were determined from the HN fits. Specifically, the relaxation times ( $\tau_{\text{MAX}}$ ) associated with the peak maxima in Fig. 6 can be derived from the HN relaxation time ( $\tau_{\text{HN}}$ ) at each temperature [35]:

$$\tau_{\text{MAX}} = \tau_{\text{HN}} \left[ \frac{\sin(\frac{\pi ab}{2+2b})}{\sin(\frac{\pi a}{2+2b})} \right]^{1/a} \quad (2)$$

For the  $\beta$  relaxation, the skewing parameter ( $b$ ) was taken as equal to 1, such that  $\tau_{\text{MAX}} = \tau_{\text{HN}}$ . The frequency maxima for the dielectric relaxations,  $f_{\text{MAX}} = [2\pi\tau_{\text{MAX}}]^{-1}$ , are plotted vs. reciprocal temperature (i.e., Arrhenius plots) in Fig. 5.

Across the  $\gamma$  relaxation range, the dielectric data follow a linear Arrhenius relation that is identical to the result from the dynamic

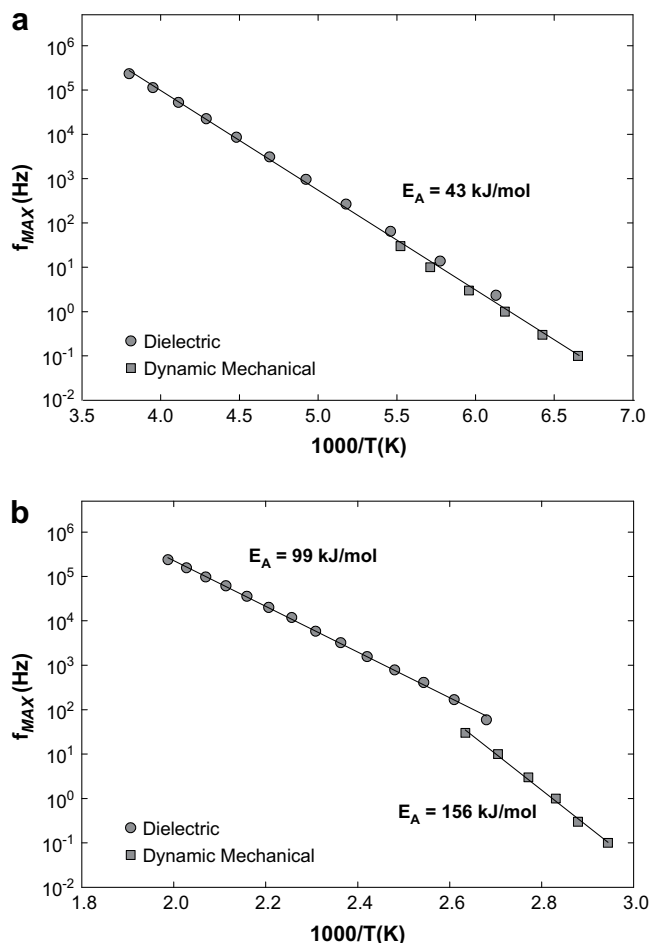


**Fig. 5.** Arrhenius plots of  $\log(f_{\text{MAX}})$  vs.  $1000/T$  (K) based on dynamic mechanical and dielectric results. (a)  $\gamma$  transition; (b)  $\beta$  transition.

mechanical studies. The combined dynamic mechanical and dielectric data span nearly seven orders of magnitude in relaxation time with an apparent activation energy of 43 kJ/mol. The consistency of the dynamic mechanical and dielectric data suggests that the DMA and BDS techniques are probing the same underlying motions. Examination of the backbone structure of the BTDA–DAPI polymer (*re*: Fig. 1) reveals that the dielectric dispersion response most likely originates from motions involving the dianhydride segment, given the concentration of permanent dipoles, as well as the potential for interactions with residual water molecules, in this portion of the repeat unit. In the case of the  $\beta$  transition, the dielectric data again show a linear Arrhenius behavior (see Fig. 5b), but the dielectric results do not match the time–temperature relation established by the dynamic mechanical measurements. For the dielectric probe,  $E_A$  ( $\beta$ ) = 99 kJ/mol, which is significantly less than the value obtained via DMA (156 kJ/mol). Further, when extrapolated to the low-frequency range, the dielectric relation predicts peak temperatures ( $T_\beta$ ) that are lower than those obtained via dynamic mechanical testing. This outcome (*i.e.*, downward offset in dielectric peak temperatures relative to dynamic mechanical result) is typical of sub-glass relaxation data obtained for a wide range of flexible and rigid polymers, as demonstrated in the extensive compilation of McCrum et al. [36].

The linear Arrhenius quality of both the  $\gamma$  and the  $\beta$  processes is indicative of a localized, relatively non-cooperative molecular origin for these relaxations that is characteristic of sub-glass polymer relaxations in general. Additional insight with respect to

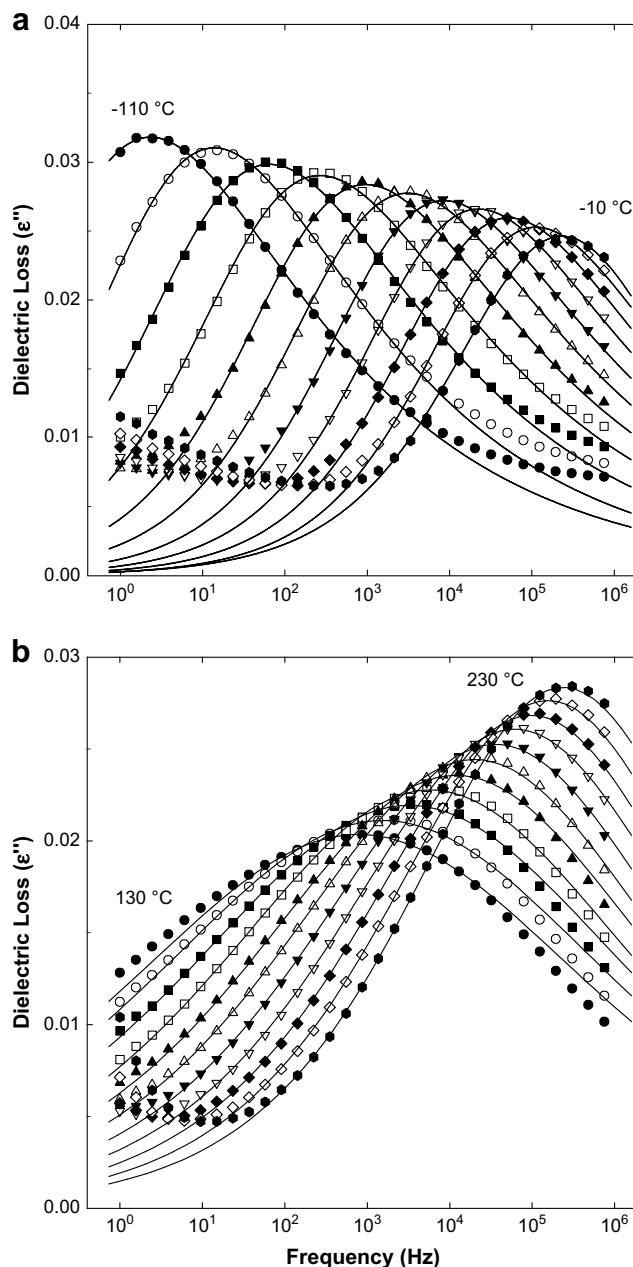


**Fig. 6.** Dielectric loss vs. frequency (Hz) for Matrimid® polyimide. (a)  $\gamma$  transition; (b)  $\beta$  transition. Data are presented at 10 °C intervals. Solid curves are Havriliak–Negami (HN) best fits to the data.

the character of sub-glass relaxations can be obtained according to the approach described by Starkweather [37,38], wherein the apparent activation energy associated with each relaxation is related to the relaxation temperature ( $T'$ ) and its corresponding activation entropy ( $\Delta S^+$ ) at a frequency of 1 Hz:

$$E_A = RT'[1 + \ln(kT'/2\pi h)] + T'\Delta S^+ \quad (3a)$$

where  $k$  is Boltzmann's constant and  $h$  is Planck's constant. For simple, non-cooperative relaxations, Starkweather suggests that  $\Delta S^+ \rightarrow 0$ , with the resulting equation providing a limiting relationship between activation energy and relaxation temperature for isolated, non-interactive motional processes:

$$E_A = RT'[1 + \ln(k/2\pi h) + \ln(T')] \quad (3b)$$

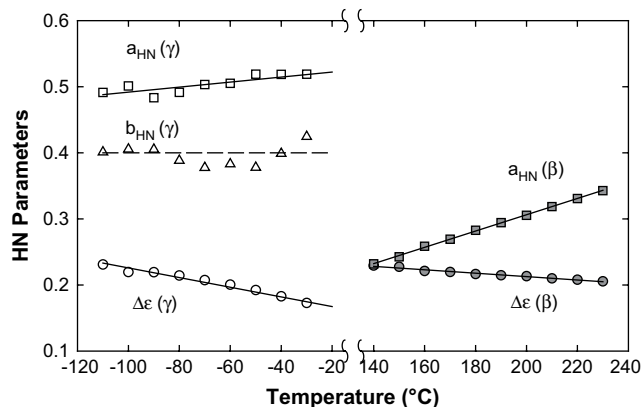


**Fig. 7.** Havriliak–Negami (HN) parameters vs. temperature (°C) for  $\gamma$  and  $\beta$  transition regions.  $a_{\text{HN}}$ : broadening parameter;  $b_{\text{HN}}$ : skewing parameter;  $\Delta\epsilon$ : dielectric relaxation intensity.

A plot of activation energy vs. temperature for the sub-glass transitions in Matrimid is presented in Fig. 8; the solid line in the plot reflects the  $\Delta S^\ddagger = 0$  non-cooperative limit. For the  $\gamma$  transition, the activation energy obtained from the DMA and BDS measurements falls very close to the zero-entropy limit, reflecting the essentially non-cooperative character of this relaxation as probed by both methods. This result is consistent with similar analyses of the polyimide  $\gamma$  process as reported in the literature [23]. For the  $\beta$  transition, two important features are evident in Fig. 8: (i) the results from the DMA and BDS measurements are positioned well above the zero-entropy line, indicating some degree of cooperative character inherent to the relaxation as detected by both techniques, and (ii) the dynamic mechanical  $E_A$  value shows a much higher degree of offset, suggesting that the DMA measurement is capable of detecting a range of motions that encompass a higher level of

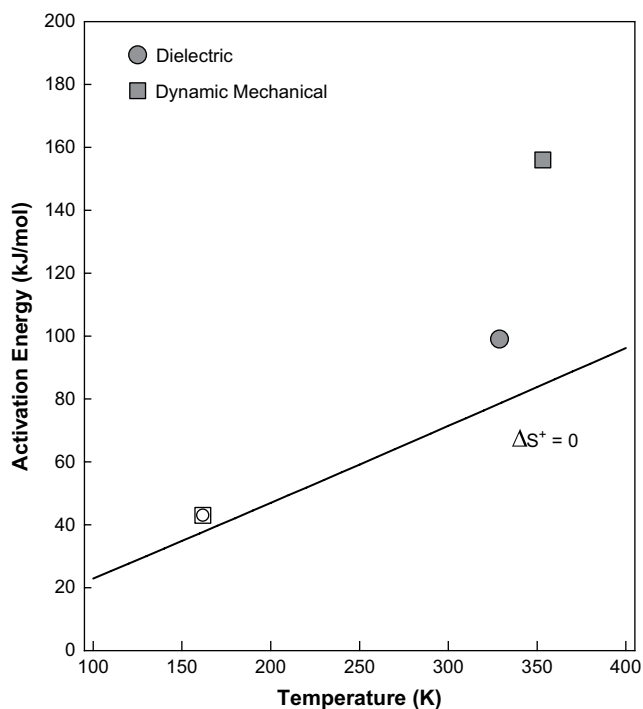


**Fig. 8.** Apparent activation energy (kJ/mol) vs. relaxation temperature (K) at 1 Hz based on dynamic mechanical and dielectric results. Solid line represents  $\Delta S^\ddagger = 0$  limit (re: Eq. (3b)). Unfilled symbols:  $\gamma$  transition. Filled symbols:  $\beta$  transition.

cooperativity as compared to the dielectric probe. Considering the structure of the Matrimid molecule and the location of permanent dipoles within the repeat unit, one possible explanation for the contrasting dielectric and dynamic mechanical results is that the measured dielectric response is limited to motions of the BTDA dianhydride segment, while the dynamic mechanical response reflects longer-range correlated motions involving both portions of the repeat unit. The longer-range motions captured by the dynamic mechanical data would likely engender a higher degree of intra- and intermolecular cooperativity, as shown in Fig. 8. The offset in activation energy reported here for the dynamic mechanical  $\beta$  transition is comparable to the results for other polyimides [23,28].

### 3.3. Glass–rubber relaxation process

Fig. 9 shows detailed dynamic mechanical results for the  $\alpha$  relaxation range; the observed two order of magnitude decrease in storage modulus is consistent with assignment of this relaxation to the glass–rubber transition. Time–temperature superposition was performed in order to obtain master curves of storage and loss moduli vs. frequency across the  $\alpha$  transition [39]. The storage modulus master curve was obtained strictly by horizontal shifting of the data and is plotted as  $E'$  vs.  $\omega a_T$  in Fig. 10a, where  $\omega$  is the applied test frequency and  $a_T$  is the dimensionless shift factor. A reference temperature of 307 °C was selected which corresponds to a central relaxation time,  $\langle\tau\rangle$ , equal to 1 s. A similar master curve for

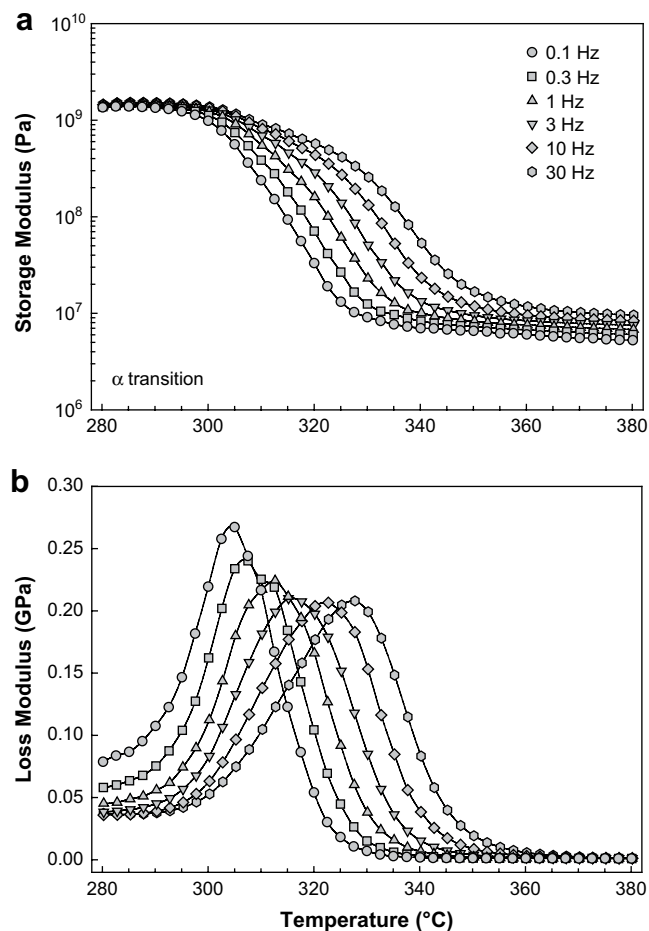


**Fig. 9.** Storage modulus and loss modulus vs. temperature (°C) for Matrimid® polyimide in the vicinity of the glass–rubber ( $\alpha$ ) relaxation.



loss modulus could be obtained by a combination of horizontal shifting (same  $a_T$  values as above) and vertical shifting; the result is shown in Fig. 10b.

Both the storage and loss master curves for the  $\alpha$  transition could be described using the Kohlrausch–Williams–Watts (KWW) “stretched exponential” relaxation time distribution function:

$$\phi(t) = \exp\left[-(t/\tau_0)^{\beta_{\text{KWW}}}\right] \quad (4)$$

where  $\tau_0$  is the relaxation time and  $\beta_{\text{KWW}}$  is the distribution or breadth parameter.  $\beta_{\text{KWW}}$  can range from 0 to 1, with  $\beta_{\text{KWW}} = 1$  corresponding to a single-relaxation time Debye response. Lower values of  $\beta$  typically reflect increased intermolecular cooperativity as influenced by the chemical structure of the polymer, as well as potential constraints owing to the presence of crystallinity or crosslinks [40]. Series approximations reported by Williams et al. express modulus and loss for the KWW model in the frequency domain, and these equations were used as the basis for the curve fits reported here [41]. The solid curves shown in Fig. 10 correspond to a single KWW fit with a corresponding distribution parameter,  $\beta_{\text{KWW}} = 0.34$ .

The time–temperature character of the glass–rubber relaxation can be assessed by the construction of a cooperativity plot, a normalized Arrhenius plot where the shift factor ( $a_T = \tau/\tau_\alpha$ ) is plotted as  $\log(a_T)$  vs.  $T_\alpha/T$  in the vicinity of the glass transition. In

this context,  $T_\alpha$  is the experimental temperature that corresponds to a central relaxation time ( $\tau_\alpha$ ) of 100 s. The cooperativity plot for Matrimid based on the dynamic mechanical results is presented in Fig. 11 with  $T_\alpha = 296^\circ\text{C}$ . The data display non-Arrhenius curvature when plotted against reciprocal temperature that is consistent with the cooperative character of the glass–rubber relaxation; the solid curve corresponds to a WLF (Williams–Landel–Ferry) best fit to the data [39].

The time–temperature sensitivity of the Matrimid polymer across the glass transition can be expressed in terms of its dynamic fragility. Polymers that display severe degradation of structure with temperature are designated as fragile liquids and their relaxation typically reflects a high level of intermolecular coupling, often as a result of a less flexible backbone or the presence of sterically cumbersome pendant groups. By contrast, polymers with smooth, more flexible backbones tend to experience reduced intermolecular constraint and as a result display less time–temperature sensitivity and correspondingly lower fragility [40]. The fragility index,  $m$ , quantifies the time–temperature sensitivity of the polymer glass transition based on the slope of the cooperativity curve evaluated at  $T = T_\alpha$ :

$$m = \left. \frac{d\log(\tau)}{d(T_\alpha/T)} \right|_{T=T_\alpha} = \left. \frac{d\log(a_T)}{d(T_\alpha/T)} \right|_{T=T_\alpha} \quad (5)$$

The value of  $m$  depends upon the definition of  $T_\alpha$ : for the glass transition, the convention is to assign  $T_\alpha$  such that the corresponding relaxation time,  $\tau(T_\alpha) = 100$  s. Values of the fragility index determined on this basis range from  $m = 16$  (strong limit) to  $m \geq 200$  (fragile limit) [42]. Tabulations of dynamic fragility have been reported in the literature for a variety of polymers and small molecules [42–44]. For simple polyethylene,  $m = 46$ , while for vinyl polymers with pendant substituents, the fragility index is considerably higher (e.g.,  $m = 137$  for polypropylene; 191 for PVC) [43]. Linear amorphous polymers with stiffer backbones also show relatively high fragility values; for polycarbonate,  $m = 132$  [42]. Based on the dynamic mechanical data presented in Fig. 11, a fragility index of  $m = 115$  is obtained for Matrimid polyimide.

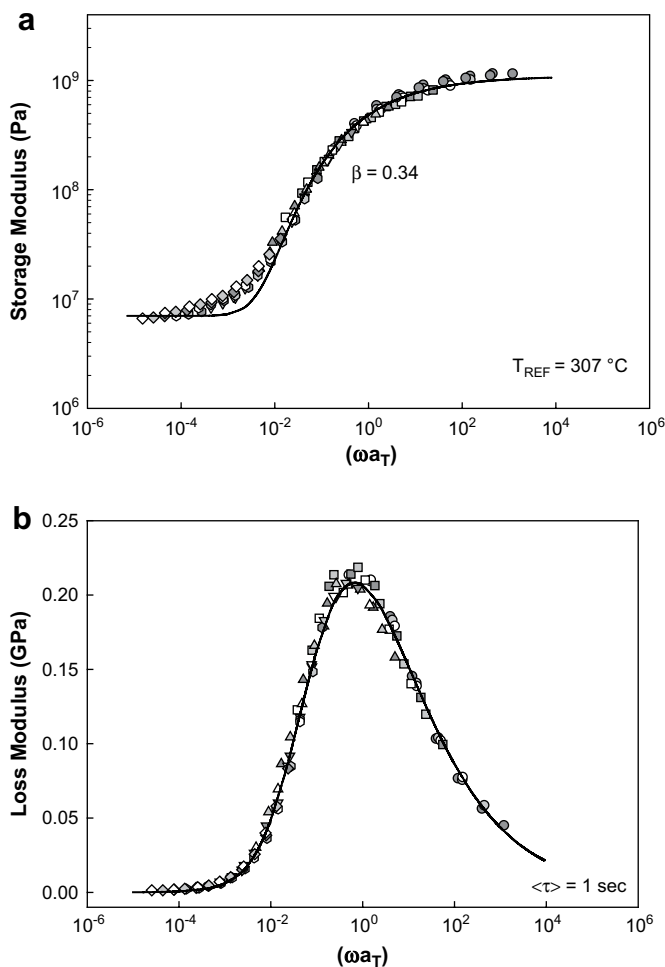


Fig. 10. Dynamic mechanical time–temperature master curves at a reference temperature of  $307^\circ\text{C}$  ( $\tau = 1$  s); glass–rubber relaxation. (a) Storage modulus; (b) loss modulus. Solid curves represent KWW best fit.

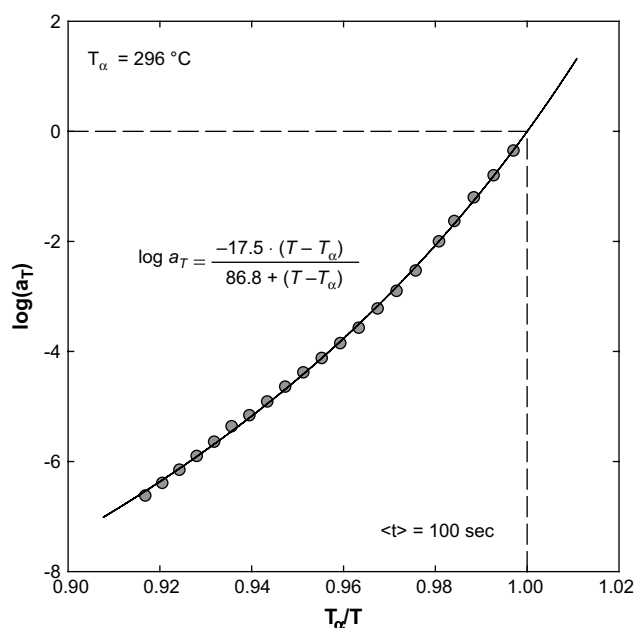


Fig. 11. Cooperativity plot of  $\log(a_T)$  vs.  $T_\alpha/T$  based on dynamic mechanical measurements.  $T_\alpha = 296^\circ\text{C}$  ( $\tau = 100$  s). Solid curve is WLF fit.

Bohmer et al. reported an inverse correlation between the fragility index ( $m$ ) and the stretching exponent ( $\beta_{\text{KWW}}$ ) that is valid across a number of material families, with higher values of  $m$  corresponding to a stronger degree of non-exponentiality (i.e., lower values of  $\beta_{\text{KWW}}$  and greater intermolecular coupling) [42]. The parameters measured for Matrimid polyimide ( $m = 115$ ;  $\beta_{\text{KWW}} = 0.34$ ) exhibit a reasonably good correspondence with the correlation bounds presented by Bohmer; examination of the values reported in Ref. [42] shows a cluster of data for a subset of polymers with  $\beta_{\text{KWW}} \sim 0.35$ , and  $m$  ranging from 120 to 145. Thus, the relatively rigid nature of the Matrimid backbone is observed to correlate with both relaxation breadth and somewhat fragile time-temperature character consistent with the overall behavior reported for a range of polymers.

#### 4. Conclusions

The dynamic relaxation properties of BTDA-DAPI (Matrimid®) polyimide were investigated using dynamic mechanical and dielectric methods. Matrimid displayed two sub-glass relaxations with increasing temperature centered at  $-112^\circ\text{C}$  ( $T_\gamma$ ) and  $80^\circ\text{C}$  ( $T_\beta$ ) based on the measured maxima in mechanical loss modulus at 1 Hz. Application of the analysis proposed by Starkweather indicated that the  $\gamma$  transition was non-cooperative in nature, and both DMA and BDS measurements provided an apparent activation energy of 43 kJ/mol that was consistent with values reported for similar polyimides. The  $\beta$  transition had a more cooperative character, and comparison of dynamic mechanical and dielectric Arrhenius data indicated a higher apparent activation energy for the DMA tests ( $E_A = 156$  kJ/mol) as compared to the BDS studies (99 kJ/mol). It was postulated that the dynamic mechanical probe was sensitive to a wider range of sub-glass motions across the  $\beta$  relaxation range encompassing a higher level of cooperative response. The glass-rubber relaxation ( $T_\alpha = 313^\circ\text{C}$ ) was evaluated by time-temperature superposition; the resulting dynamic mechanical master curves were fit using the KWW stretched exponential function, with a corresponding exponent  $\beta_{\text{KWW}} = 0.34$ . A cooperativity plot was used to establish the dynamic fragility of the polymer. The value of the fragility index ( $m = 115$ ) reflected the relatively rigid character of the polyimide backbone, and the observed relation between fragility and  $\beta_{\text{KWW}}$  was consistent with the correlation reported in the literature for a wide variety of polymers.

#### Acknowledgments

Acknowledgment is made to the Donors of the American Chemical Society Petroleum Research Fund (PRF #45353-AC7) for partial support of research activities conducted at the University of Kentucky. In addition, we are pleased to acknowledge the assistance of Dr. Matthew Weisenberger of the University of Kentucky Center for Applied Energy Research in the performance of the dynamic mechanical measurements. Research activities at the

University of Texas at Austin were supported by the National Science Foundation (Grant DMR-0238979 administered by the Division of Materials Research-Polymers Program) and by Air Liquide/Medal.

#### References

- [1] Struik LCE. Physical aging in amorphous polymers and other materials. Amsterdam: Elsevier; 1978.
- [2] Hutchinson JM. Prog Polym Sci 1995;20:703–60.
- [3] Hodge IM. Science 1995;267:1945–7.
- [4] Drozdov AD. J Appl Polym Sci 2001;81:3309–20.
- [5] Venditti RA, Gillham JK. J Appl Polym Sci 1992;45:1501–16.
- [6] Lee HHD, McGarry FJ. Polymer 1993;34:4267–72.
- [7] Bateman J, Gordon DA. US Patent 3,856,752; 1974.
- [8] Bos A, Punt IGM, Wessling M, Strathmann H. Sep Purif Technol 1998;14:27–39.
- [9] Ekiner OM. US Patent 5,015,270; 1991.
- [10] Simmons JW, Ekiner OM. US Patent 5,232,472; 1993.
- [11] Madden WC, Punsalan D, Koros WJ. Polymer 2005;46:5433–6.
- [12] Huang Y, Paul DR. Polymer 2004;45:8377–93.
- [13] Huang Y, Paul DR. Macromolecules 2006;39:1554–9.
- [14] Lim T, Frosini V, Zaleckas V, Morrow D, Sauer JA. Polym Eng Sci 1973;13:51–8.
- [15] Perena JM. Angew Makromol Chem 1982;106:61–6.
- [16] Xu G, Gryte CC, Nowick AS, Li SZ, Pak YS, Greenbaum SG. J Appl Phys 1989;66:5290–6.
- [17] Sun Z, Dong L, Zhuang Y, Cao L, Ding M, Feng Z. Polymer 1992;33:4728–31.
- [18] Arnold Jr FE, Bruno KR, Shen D, Eashoo M, Lee CJ, Harris FW, et al. Polym Eng Sci 1993;33:1373–80.
- [19] Coburn JC, Soper PD, Auman BC. Macromolecules 1995;28:3253–60.
- [20] Cheng SZD, Chalmers TM, Gu Y, Yoon Y, Harris FW, Cheng J, et al. Macromol Chem Phys 1995;196:1439–51.
- [21] Kim YH, Moon BS, Harris FW, Cheng SZD. J Therm Anal 1996;46:921–33.
- [22] Habas JP, Peyrelasse J, Grenier-Loustalot MF. High Perform Polym 1996;8:515–32.
- [23] Li S, Hsu BL, Li F, Li CY, Harris FW, Cheng SZD. Thermochim Acta 1999;340–341:221–9.
- [24] Li F, Fang S, Ge JJ, Honigfort PS, Chen JC, Harris FW, et al. Polymer 1999;40:4571–83.
- [25] Li F, Ge JJ, Honigfort PS, Fang S, Chen J-C, Harris FW, et al. Polymer 1999;40:4987–5002.
- [26] Qu W, Ko TM, Vora RH, Chung TS. Polymer 2001;42:6393–401.
- [27] Eichstadt AE, Ward TC, Bagwell MD, Farr IV, Dunson DL, McGrath JE. Macromolecules 2002;35:7561–8.
- [28] Bas C, Tamagna C, Pascal T, Alberola ND. Polym Eng Sci 2003;43:344–55.
- [29] Ngai KL, Paluch M. J Chem Phys 2004;120:857–73.
- [30] Rowe B. Ph.D. Thesis. Austin, TX: The University of Texas at Austin; 2009.
- [31] Rowe BW, Freeman BD, Paul DR. Macromolecules 2007;40:2806–13.
- [32] Havriliak S, Negami S. J Polym Sci Polym Symp 1966;14:99–103.
- [33] Havriliak S, Havriliak SJ. Dielectric and mechanical relaxation in materials. Cincinnati: Hanser; 1997.
- [34] Cole KS, Cole RH. J Chem Phys 1941;9:341–51.
- [35] Schonhals A, Kremer F. Analysis of dielectric spectra. In: Kremer F, Schonhals A, editors. Broadband dielectric spectroscopy. Berlin: Springer-Verlag; 2003. p. 59–98.
- [36] McCrum NG, Read BE, Williams G. Anelastic and dielectric effects in polymeric solids. London: John Wiley and Sons; 1967.
- [37] Starkweather HW. Macromolecules 1981;14:1277–81.
- [38] Starkweather HW. Polymer 1991;32:2443–8.
- [39] Ferry JD. Viscoelastic properties of polymers. 3rd ed. New York: John Wiley and Sons; 1980.
- [40] Ngai KL, Roland CM. Macromolecules 1993;26:6824–30.
- [41] Williams G, Watts DC, Dev SB, North AM. Trans Faraday Soc 1971;67:1323–35.
- [42] Bohmer R, Ngai KL, Angell CA, Plazek DJ. J Chem Phys 1993;99:4201–9.
- [43] Roland CM, Santangelo PG, Ngai KL. J Chem Phys 1999;111:5593–8.
- [44] Huang D, McKenna GB. J Chem Phys 2001;114:5621–30.